2018 IEEE International Conference on Systems, Man, and Cybernetics

Motion Planning Strategies and Human Performance in the Manipulation of Underactuated Flexible Objects

Mikhail Svinin, Evgeni Magid, Igor Goncharenko, and Victor Kryssanov

Abstract— **The paper deals with modeling of human-like reaching movements in dynamic environments. A simple but not trivial example of reaching in a dynamic environment is the rest-to-rest manipulation of a multi-mass flexible object with the elimination of residual vibrations. In this movement task, the hand velocity profiles may have a form that is quite different from the classical bell shape. Two approaches to the prediction of reaching movements are formulated in position and force actuation settings. In the first approach, either the position of the hand or the hand force is specified by the lowest order polynomial satisfying the boundary conditions of the reaching task. The second approach is based on the minimization of either the hand jerk or the hand force-change, with taking into account the dynamics of the flexible object. To verify the resulting four mathematical models, an experiment on the manipulation of a ten-masses flexible object of low stiffness is conducted. The experimental results show that the second approach gives a significantly better prediction of human movements, with the minimum hand force-change model having an edge over the minimum hand jerk one.**

Index Terms— **Human-like reaching movements, dynamic environment, flexible objects, optimality.**

I. Introduction

Modeling of human-like reaching movements is an important research problem in biological motor control and cybernetics [1]–[3]. From the viewpoint of control theory the problem can be approached from two directions: one focuses on the feedforward control [4], and another is based on the feedback control [5]. In this paper we will deal with the feedforward control of reaching movements. In this approach, the trajectory of the human hand is often predicted by minimizing an integral criterion subject to boundary conditions imposed on start and end points. It is well established that for the unconstrained reaching movements the trajectory of human hand can be predicted with reasonable accuracy by the minimum hand jerk (MHJ) [6] and the minimum joint torque change [7] criteria.

While the optimization models are not fully accurate, they can capture the invariant features of unconstrained reaching movements, in particular the bell-shaped velocity profile [8], [9], reasonably well. However, this can be done by a variety of functional relations [10] not necessarily based on the optimization models. In this connection, the design of critical tests for reaching tasks, featuring not only a single-peaked bell shape but more complex shapes of the hand velocity profiles, is a very important research problem [11]. To approach this problem, one can "place" the human hand in an artificially created dynamic environment.

An example of reaching in a dynamic environment is the rest-to-rest manipulation of a linear chain of flexible objects with the suppression of structural vibrations at the end of movement. Despite the seeming simplicity, this task requires a lot of skill that must be acquired through practicing. The difficulty stems from the fact that the system under control is under-actuated. It has multiple degrees of freedom controlled by a single input. An interesting feature of this task, first observed in experiments with one-mass flexible object [12], is that under certain conditions the human controls the object in a non-trivial way, keeping two distinct phases in the hand velocity profile.

Considering this manipulation task from the control engineering point of view, one can employ different strategies to generate rest-to-rest motion commands that eliminate residual vibrations [13], [14]. Perhaps the simplest open-loop control strategy is to specify the motion of the most distal link of the flexible object by the lowest order polynomial (LOP) satisfying the boundary conditions [15], [16]. This control strategy has been successfully applied to modeling of reaching movements in the manipulation of one flexible object [12]. However, it does not capture well the velocity profiles of reaching movements in the case of multi-mass flexible objects, and is less consistent in comparison with the MHJ model [17].

Another possible strategy to plan the reaching movement with the flexible object is to specify by the LOP the motion of not the most distal link but the foremost link that is the hand. It is known that the MHJ model of reaching movement in the free space is mathematically equivalent to matching by the LOP the boundary conditions imposed on the hand position, velocity and acceleration [6]. However, as will be shown in this paper, the LOP strategy and the strategy based on the minimization of the control effort (the hand jerk) are not mathematically equivalent for reaching movements in dynamic environments. It is, therefore, of interest to compare these strategies of the hand trajectory formation and examine how well they capture the patterns of human movements.

It should be noted that the above specified two movement strategies can be formulated in kinematic (as discussed above) or dynamic (when the inertia of the human hand is not ignored) settings, resulting into four computational models. The dynamic counterpart of the MHJ model is the minimum hand force-change (MHFC) model. Likewise, the dynamic equivalent of the kinematic LOP model is the LOP specification of the hand driving force. It is interesting to note that the

M. Svinin, I. Goncharenko, and V. Kryssanov are with the College of Information Science and Engineering, Ritsumeikan University, 1-1-1 Nojihigashi, Kusatsu, Shiga 525-8577, Japan, svinin@fc.ritsumei.ac.jp, E. Magid is with the Intelligent Robotics Department, Higher School of Information Technology and Information Systems, Kazan Federal University, Kazan, Russian Federation, magid@it.kfu.ru

2577-1655/18/$31.00 ©2018 IEEE
DOI 10.1109/SMC.2018.00586

latter model can be linked to the definition of natural motion in analytical mechanics [18] and to the Gauss principle of least constraint for the control of mechanical systems [19]. In this connection, it is worthwhile to investigate how this formal way of the construction of natural motion works in the context of natural human movements. This constitutes the goal of this paper.

The paper is organized as follows. In Section II, we formalize a mathematical description of the flexible object and the boundary conditions for the reaching task. In Section III we establish the mathematical structure of four theoretical models. Analytical solutions provided by these models are tested against experimental data in Section IV which also describes the experimental setup and the protocol of collecting the data. Conclusions are summarized in Section V.

II. Model of the dynamic environment

In this section we formalize reaching movements in a dynamic environment that is modeled as a multi-mass flexible object. For the sake of simplicity, we deal with a one-dimensional model of human movements. In this model the configuration dependance of the human arm is ignored and the motion is considered at the hand level.

A. System dynamics

Assume that the object to be manipulated is composed of n beads of mass m connected by n springs of stiffness coefficient k as shown in Figure 1. For the uniform mass and and stiffness distribution, the dynamic equations can be written down as follows

$$\begin{aligned} m_0\ddot{x}_0 + k(x_0 - x_1) &= f, & (1)\\ m\ddot{x}_s + k(x_s - x_{s-1}) + k(x_s - x_{s+1}) &= 0, & (2)\\ m\ddot{x}_n + k(x_n - x_{n-1}) &= 0, & (3)\end{aligned}$$

where x_s, $s = 1, \ldots, n$, are the positions of the beads, x_0 stands for the position of the hand, m_0 is the hand mass, and f is the driving force.

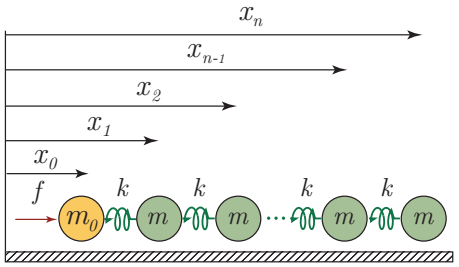

Fig. 1. Multi-mass flexible object driven by the hand.

For establishing trajectory formation models it is convenient to represent the system's dynamics in terms of the object end position x_n and its derivatives. By solving equations (2,3) recurrently for $s = n-1, n-2, \ldots, 1$, one obtains [17]:

$$\sum_{l=0}^{s} \frac{C_{s+l}^{s-l}}{\omega^{2l}}\, x_n^{(2l)}(t) = x_{n-s}(t), \qquad (4)$$

where $C_p^q = p!/(q!(p-q)!)$ denotes the binomial coefficients, $x_n^{(2l)}$ stands for the $2l$-th time derivative of the n-th coordinate, and $\omega = \sqrt{k/m}$.

By setting $s = n$ in (4), one converts the system of n differential equations of the 2nd order (2,3) to one differential equation of the $2n$-th order

$$\sum_{l=0}^{n} \frac{C_{n+l}^{n-l}}{\omega^{2l}}\, x_n^{(2l)}(t) = x_0(t), \qquad (5)$$

which describes the dynamics of flexible object under kinematic actuation by the hand position x_0.

By combining (5), (1), and (4) taken for $s = n-1$, one converts the system of $n+1$ differential equations of the 2nd order (1,2,3) to one differential equation of the $2(n+1)$-th order

$$\sum_{l=0}^{n} \frac{C_{n+l}^{n-l}}{\omega^{2l}} \left\{ m_0 x_n^{(2l+2)}(t) + \frac{2lk}{n+l} x_n^{(2l)}(t) \right\} = f(t), \qquad (6)$$

which describes the dynamics of the combined system, composed of the hand and the flexible object, driven by the hand force f.

B. Reaching task and the boundary conditions

Assume that a human subject makes a reaching movement of length L and time T and stops at the target point the hand and all the beads of the object without excitation of oscillations. Without loss of generality we assume that the subject transports all the beads from the initial state

$$x_s(0) = 0,\ \dot{x}_s(0) = 0, \quad s = 1, \ldots, n, \qquad (7)$$

to the final state

$$x_s(T) = L,\ \dot{x}_s(T) = 0, \quad s = 1, \ldots, n. \qquad (8)$$

Assuming that the hand is at rest in the beginning and in the end of the reaching movement, one has

$$\begin{aligned} x_0(0) = 0, \quad \dot{x}_0(0) = 0, \quad \ddot{x}_0(0) = 0, & \qquad (9)\\ x_0(T) = L, \quad \dot{x}_0(T) = 0, \quad \ddot{x}_0(T) = 0. & \qquad (10)\end{aligned}$$

In what follows, we will derive trajectory formation models in terms of the object end position and for this purpose we need to formulate the boundary conditions for $x_n(t)$ and its higher derivatives. They can be obtained from the boundary conditions (7,8) and (9,10). Differentiating equations (2,3) sequentially, s-th equation $2s$ times, and considering them at $t = 0$ and $t = T$, one obtains

$$\begin{aligned} x_s^{(2)}(0) = x_s^{(3)}(0) = \quad \ldots = x_s^{(2s+2)}(0) = 0, & \qquad (11)\\ x_s^{(2)}(T) = x_s^{(3)}(T) = \quad \ldots = x_s^{(2s+2)}(T) = 0. & \qquad (12)\end{aligned}$$

Combining (7,8) and (11,12) for $i = n$, one establishes the boundary conditions for the object end position:

$$\begin{aligned} x_n(0) = 0, \quad \dot{x}_n(0) = \ldots = x_n^{(2n+2)}(0) = 0, & \qquad (13)\\ x_n(T) = L, \quad \dot{x}_n(T) = \ldots = x_n^{(2n+2)}(T) = 0. & \qquad (14)\end{aligned}$$

In total, we have $2(2n+3)$ boundary conditions.

III. Motion planning strategies

In this section, we outline two motion planning strategies for the reaching task under consideration. One is based on the LOP representation of the control input, and another one is based on the minimization of the squared control effort integrated over the movement duration.

For each of the strategies we will consider two types of actuation, position-based and force-based. For the position-based actuation, the actuator dynamics (i.e., the hand dynamics (1)) do not play an independent role in establishing motion trajectories, and are not included in model (5). It is thus assumed that the human arm, controlled by the CNS, is an ideal actuator driving the hand in the task space. Under such an assumption inertial properties of the arm are not taken into consideration [6].

For the force-based actuation the hand dynamics (1) and the hand mass are included in model (6). It is thus assumed that the CNS does take into account inertial properties of the arm [7]. The hand driving force is directly involved in establishing motion trajectories while in the position-based actuation it is estimated after the motion trajectories have been established.

A. LOP strategy: position-based actuation

The dynamics of the last bead in (5) are actuated by the hand position x_0. One way to plan reaching movements for the task defined in Section II-B is to specify the motion of the hand, $x_0(t)$, in the form of the LOP satisfying the boundary conditions (13,14). For $x_0(t) = 0$ equation (5) has $2n$ integration constants. The total number of the boundary conditions (13,14) is $2(2n + 3)$. Therefore, the differential equation for the lowest order polynomial control input $x_0(t)$ must have the order $2(2n+3) - 2n = 2n+6$. Thus, one has $x_0^{(2n+6)}(t) = 0$ and therefore

$$x_0(t) = \sum_{i=0}^{2n+5} a_i\, t^i, \tag{15}$$

where a_i are unknown constant coefficients.

By differentiating (5) $2n + 6$ times, one obtains the following linear differential equation

$$\sum_{s=0}^{n} \frac{C_{n+s}^{n-s}}{\omega^{2s}}\, x_n^{(2(n+s)+6)}(t) = 0. \tag{16}$$

Its characteristic equation has $2n + 6$ zero roots and n pairs of imaginary roots $\pm\imath\, p_s$, where $p_s,\ s = 1, 2, \ldots, n$, are the natural frequencies of the flexible object The trajectory of the last bead is therefore defined as

$$x_n(t) = \sum_{i=0}^{2n+5} \alpha_i t^i + \sum_{i=1}^{n} \beta_i \sin(p_i t + \gamma_i), \tag{17}$$

where the $4n + 6$ coefficients $\alpha_i, \beta_i, \gamma_i$ are calculated from the $4n + 6$ boundary conditions (13,14). The substitution of (17) into (5) results in a pure polynomial form, from which one can find the coefficients a_i in (15).

B. LOP strategy: force-based actuation

This strategy is closely related to the approach for generation of human-like reaching movements based on the modified Hamilton principle and on the definition of natural systems adopted in analytical mechanics [18].

The dynamics of the last bead in (6) are actuated by the hand force f. For $f(t) = 0$ equation (6) has $2(n + 1)$ integration constants. The total number of the boundary conditions (13,14) is $2(2n + 3)$. Therefore, the differential equation for the lowest order polynomial control input $x_0(t)$ must have the order $2(2n + 3) - 2(n + 1) = 2n + 4$. Thus, one has $f^{(2n+4)}(t) = 0$ and therefore

$$f(t) = \sum_{i=0}^{2n+3} f_i\, t^i, \tag{18}$$

where f_i are unknown constant coefficients.

By differentiating (6) $2n + 4$ times, one obtains the following linear differential equation:

$$\sum_{l=0}^{n} \frac{C_{n+l}^{n-l}}{\omega^{2l}} \left\{ x_n^{(2(n+l)+6)}(t) + \frac{2l\mu\omega^2}{n+l} x_n^{(2(n+l)+4)}(t) \right\} = 0, \tag{19}$$

where the mass ratio $\mu = m/m_0$. The characteristic equation corresponding to (19) has $2n + 6$ zero roots and n pairs of imaginary roots $\pm\imath\,\tilde{p}_s$, where $\tilde{p}_s,\ s = 1, 2, \ldots, n$, are the natural frequencies of the combined (hand & flexible object) system. The trajectory of the last bead is therefore defined as

$$x_n(t) = \sum_{i=0}^{2n+5} \alpha_i t^i + \sum_{i=1}^{n} \beta_i \sin(\tilde{p}_i t + \gamma_i), \tag{20}$$

where the $4n + 6$ coefficients $\alpha_i, \beta_i, \gamma_i$ are defined from the $4n + 6$ boundary conditions (13,14). Since the natural frequencies $\tilde{p}_i$ differ from p_i, the structure of the hand trajectory x_0 mimics that of x_n:

$$x_0(t) = \sum_{i=0}^{2n+5} a_i t^i + \sum_{i=1}^{n} b_i \sin(\tilde{p}_i t + c_i), \tag{21}$$

where coefficients a_i, b_i, c_i are obtained by plugging (20) into (5).

C. Minimum control effort strategy: the MHJ model

Consider now the MHJ model in which the system trajectories are defined by minimizing the criterion

$$J = \frac{1}{2} \int_0^T \left(\frac{\mathrm{d}^3 x_0}{\mathrm{d}t^3} \right)^2 \mathrm{d}t. \tag{22}$$

Differentiating the hand position (5) three times and substituting the result into (22), one obtains

$$J = \frac{1}{2} \int_0^T \left(\sum_{l=0}^{n} \frac{C_{n+l}^{n-l}}{\omega^{2l}}\, x_n^{(2l+3)} \right)^2 \mathrm{d}t. \tag{23}$$

Denote by $\mathcal{L}$ the integrand of criterion (23). The trajectory $x_n(t)$ minimizing J under the boundary conditions (13,14) must satisfy the Euler-Lagrange equation

$$\sum_{k=0}^{2n+3} (-1)^k \frac{\mathrm{d}^{(k)}}{\mathrm{d}t^{(k)}} \left\{ \frac{\partial \mathcal{L}}{\partial x_n^{(k)}} \right\} = 0. \tag{24}$$

For the given structure of $\mathcal{L}$, (24) reduces to the following linear differential equation:

$$\sum_{s=0}^{n}\sum_{l=0}^{n}\frac{C_{n+s}^{n-s}\,C_{n+l}^{n-l}}{\omega^{2s}\,\omega^{2l}}\,x_n^{(2\{l+s+3\})}=0. \tag{25}$$

It can be shown that the characteristic equation corresponding to (25)

$$\lambda^6\left(\sum_{s=0}^{n}\frac{C_{n+s}^{n-s}}{\omega^{2s}}\,\lambda^{2s}\right)^2=0. \tag{26}$$

has 6 zero roots and $2n$ pairs of imaginary roots $\pm\imath\,p_s$, where $p_s,\ s=1,2,\ldots,n$, are the natural frequencies of the flexible object.The optimal trajectory of the last bead is therefore defined as

$$x_n(t)=\sum_{i=0}^{5}\alpha_i\,t^i+\sum_{i=1}^{n}\beta_i\sin(p_it+\gamma_i)+t\,\delta_i\sin(p_it+\varepsilon_i), \tag{27}$$

where constant coefficients $\alpha_i,\beta_i,\gamma_i,\delta_i,\varepsilon_i$ are found from the boundary conditions (13,14).

To find the hand trajectory $x_0(t)$, one takes the even derivatives of (27) and substitute them into (5). The secular terms featured in the second sum of (27) then disappear, and the structure of the hand trajectory is defined as

$$x_0(t)=\sum_{i=0}^{5}a_i\,t^i+\sum_{i=1}^{n}b_i\sin(p_it+c_i), \tag{28}$$

where a_i,b_i,c_i are constant coefficients. Thus, the optimal hand trajectory is composed of a 5-th order polynomial (as in the classical MHJ model of reaching movements in free space [6]) and additional trigonometric terms.

D. Minimum control effort strategy: the MHFC model

In the MHFC model the system trajectories are defined by minimizing the criterion

$$J=\frac{1}{2}\int_0^T\left(\frac{\mathrm{d}f}{\mathrm{d}t}\right)^2\mathrm{d}t. \tag{29}$$

Differentiating the hand force (6) and substituting the result into (29), one obtains

$$J=\frac{m_0^2}{2}\int_0^T\left(\sum_{l=0}^{n}\frac{C_{n+l}^{n-l}}{\omega^{2l}}\left\{x_n^{(2l+3)}+\frac{2l\mu\omega^2}{n+l}x_n^{(2l+1)}\right\}\right)^2\mathrm{d}t. \tag{30}$$

Denote by $\mathcal{L}$ the integrand of criterion (30). The trajectory $x_n(t)$ minimizing criterion (30) under the boundary conditions (13,14) must satisfy the Euler-Lagrange equation (24) which, for the given structure of $\mathcal{L}$, reduces to the following linear differential equation:

$$\sum_{s=0}^{n}\sum_{l=0}^{n}\frac{C_{n+s}^{n-s}\,C_{n+l}^{n-l}}{\omega^{2s}\,\omega^{2l}}\times \\ \times\left\{x_n^{(2\{l+s+3\})}+\frac{2(l+s)\mu\omega^2}{n+l+s}x_n^{(2\{l+s+1\})}\right\}=0. \tag{31}$$

The characteristic equation corresponding to (31) has 6 zero roots and $2n$ pairs of imaginary roots $\pm\imath\,p_s^*$, where $p_s^*,\ s=1,2,\ldots,n$, are the natural frequencies of the combined (hand & flexible object) system. The optimal trajectory of the last bead is therefore defined as

$$x_n(t)=\sum_{i=0}^{5}\alpha_i\,t^i+\sum_{i=1}^{n}\beta_i\sin(p_i^*t+\gamma_i)+t\,\delta_i\sin(p_i^*t+\varepsilon_i), \tag{32}$$

where the constant coefficients $\alpha_i,\beta_i,\gamma_i,\delta_i,\varepsilon_i$ are found from the boundary conditions (13,14). The optimal hand trajectory is then obtained upon substitution of (32) into (5), which results in

$$x_0(t)=\sum_{i=0}^{5}a_i\,t^i+\sum_{i=1}^{n}b_i\sin(p_i^*t+c_i)+td_i\sin(p_i^*t+e_i), \tag{33}$$

where a_i,b_i,c_i are constant coefficients. Note that the obtained expression for the hand trajectory differs structurally from the one developed for the MHJ model.

IV. Experiment

A. Experimental Setup

To analyze velocity profiles of reaching movements with multi-mass objects, an experiment was conducted. In the experimental setup (see Figure 2), an impedance-type haptic device (PHANToM Premium 151A/3DOF by SensAble Technologies) was used to generate real-time forces (maximum exertable force 8.5N). The haptic device was connected to a computer (dual core CPU (Intel Pentium 4, 3.0 GHz)) through a PCI interface.

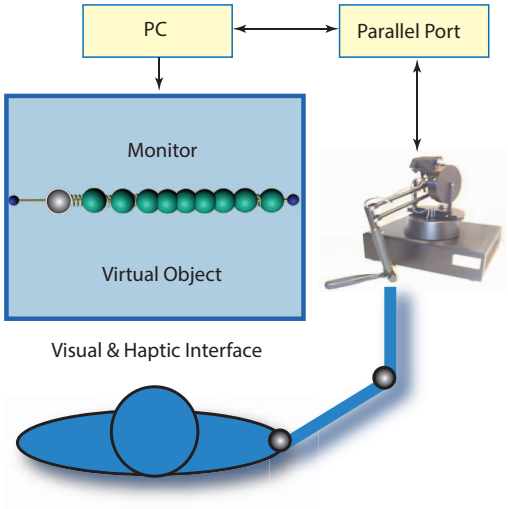

Fig. 2. Experimental setup.

Five naïve right-handed subjects (males, aged between 25 and 35 years old) participated in the experiments. The subjects were instructed to move a multi-mass virtual flexible object, with the first mass (shown black in Figure 2) "connected" to the human hand by the haptic feedback generated by the PHANToM motors. The hand & object system was at rest at the start point. Before starting movements, the subject positioned the PHANToM pointer to the first bead and "connected" it to the hand (proxy point) by pressing a button on the computer keyboard. When recording the motion data, the subject pressed another button by the left

hand and, at the same time, initiated the movement by the right hand.

The subjects were requested to move the flexible object and stop the hand and all the beads at a target point. The subjects made these rest-to-rest movements along a line (in the direction from left to right) in the horizontal plane using the PHANToM stylus. The one-dimensional movements were implemented in software by setting a higher constraint force in the directions orthogonal to the movement line. This force was realized by introducing a virtual spring (stiffness coefficient 600N/m), acting in the lateral directions. The haptic force acting along the movement line was computed as $k(x_1 - x_0)$, where x_0 is the position of the proxy (human hand) on the movement line, and x_1 is the position of the first bead of the object.

The positions of the hand and the beads were displayed on the computer monitor, providing the subject with real-time visual feedback. The object dynamics were simulated by using the conventional 4th-order Runge-Kutta method with constant step $h = 0.001\text{s}$, and the real-time haptic feedback was supplied to the subject through the PHANToM stylus. The hand position and velocity were measured by the PHANToM hardware.

B. Experimental Protocol

As the reaching movements under consideration are quite different from what one experiences in daily life, the experiment was conducted in three days. On the preliminary day we conducted a general evaluation of the subject performance. The subjects familiarized themselves with the experimental setup, comprehended the reaching task, performed movement trials, and learned the unusual dynamic environment. The subjects were asked to produce reaching movements in a natural way, on their own pace, trading off the speed (as fast as possible) and the comfort (as comfortable as possible).

A movement trial was considered successful if the task was completed within certain position and velocity tolerances. The subject was given an audio feedback, generated by the computer, when a trial was successful. No data were recorded during the preliminary evaluation as the main purpose was to select such parameters of the movement task that would guarantee an acceptable success rate and facilitate the learning process.

In the course of the preliminary experiments, we selected a flexible object of the total mass 3kg and the total stiffness 10N/m. The number of beads was set as $n = 10$, which resulted in $m = 0.3\text{kg}$ and $k = 100\text{N/m}$. For the subsequent analysis we selected the reaching task with the traveling distance $L = 0.2\text{m}$ and the movement time $T = 2.35\text{s}$. For the selected parameters, it was observed that in successful trials the subjects produced a somewhat unified movement strategy (see Figure 3) that can be qualitatively described as follows. In the beginning, the positions of all the beads coincide at the start point. During the first half of the movement, the first (driving) bead is ahead of the last (most distal) bead, with the distance between them being about 5cm. During the second half of the movement the configuration is reversed symmetrically—the driving bead becomes placed behind the last one and, finally, all the beads reach the target point.

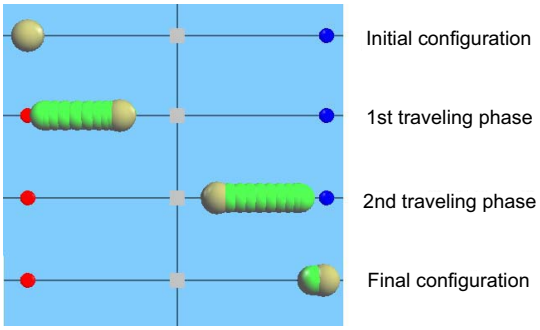

Fig. 3. A typical movement strategy observed in the preliminary trials.

To verify the observed movement strategy with a quantitative analysis, the parameters of the reaching task were subjected to tolerances. The reaching time tolerance was set as $\Delta T = \pm 0.45\text{s}$. The position and velocity tolerances to be satisfied at the start and end points we selected as $\Delta x = \pm 0.012\text{m}$ and $\Delta v = \pm 0.024\text{m/s}$ (for each of the beads), and $\Delta x = \pm 0.012\text{m}$ and $\Delta v = \pm 0.05\text{m/s}$ (for the hand). A movement trial now was considered successful if the subject was able to complete the reaching task within the tolerances specified above.

Having selected the parameters of the reaching task, we conducted further experiments in two days. On the first day, the subjects performed the reaching task and completed 600 trials. The subjects were provided with an audio feedback generated by the computer when a trial was successful. In addition, to facilitate the perception of the task timing, a time bar was displayed on the computer monitor.

The experiment was divided into two blocks. Upon completing the first 300 trials (1st block) the subjects rested for about 30 minutes and then produced another 300 trials (2nd block). The overall success rate achieved on the first day of the experiment is shown in Table I. On the second day (the recording phase) the experiment was repeated in the same order and the subjects produced another set of 600 trials. The position and velocity of the hand and those of the simulated beads were collected for analysis. These data were recorded at the sampling frequency of 100 Hz.

Having completed the main set of trials in reaching movements, the subjects rested for about one hour and then were engaged in a completely different experiment where they simply followed a periodic force produced by the PHANToM device along the same line of constraint as in the reaching movements. The purpose of this additional experiment was to identify the effective hand mass m_0 for the use in the MHFC and the dynamic LOP models. Details of this experiment are described in Appendix, and results are reported in Table II.

C. Experimental Results: Learning History

The numbers of successful trials achieved by each subject and the corresponding success rates are listed in Table I. The resulting success rates are still far from perfect after two days of practicing, that can be attributed to the complexity of the reaching task requiring a high-level of coordination skills.

However, the dynamics of the success rate shown in Figure 4 indicate that after certain numbers of trials the success rate appears to reach a plateau. The correlation between practice and performance on the learning curves is certainly not linear but rather exponential. This pattern holds for all the subjects and is, in a reasonable approximation, compatible with the classic power low of practice [20].

TABLE I

NUMBER OF SUCCESSFUL TRIALS AND THE SUCCESS RATE [%].

Subject	S1	S2	S3	S4	S5
Successful trials	122	162	173	176	219
Success rate [%]	10.17	13.50	14.41	14.67	18.25

The apparent stabilization of the success rates at relatively low values may highlight the limits of the motor skills that can be developed within the adopted experimental protocol. It should be noted that the protocol is based on the unsupervised learning paradigm where the subject is supposed to increase his motor skill based on his own experience, reinforcing it upon producing successful trials. To increase the success rates, one might need to employ supervised learning. However, this consideration remains speculative as no trainer was available for teaching the subjects.

D. Experimental Results: Velocity Profiles

Despite the relatively low success rates, the total number of successful trials is not small and is, in our opinion, acceptable for conducting a comparative analysis of the experimental and theoretical motion profiles. To compare motions of different durations, the velocity profiles of the hand and the last bead of the object were time scaled using the average time of all the successful trials, $T = 2.259$s. The data of the last ten successful trials of each subject were taken for the comparison with the theoretical predictions. Experimental velocity profiles of the hand and the last bead are presented in Figure 5. The mean values are plotted with dark green and contoured by the plus/minus standard deviation tubes shown with the light green color.

The average values of the effective hand mass m_0 (refer to Table II of Appendix D) were used in computing the corresponding theoretical profiles. The predictions by the MHJ and MHFC models are shown in Figure 5 with, respectively, the blue and red lines. The predictions by the kinematic and dynamic LOP models are shown with, respectively, the solid gray and dashed black lines. It is observed that, despite fundamental differences in the definitions, the two LOP models result in almost identical predictions for the estimated hand masses and the selected parameters of the flexible object and the reaching task.

As can be seen from Figure 5, all the theoretical models under consideration qualitatively capture the basic tendencies of human movements in the manipulation of the flexible object. In particular, the models predict the bell-shaped profiles for the velocity of the last bead of the object and the two-phased profiles for the hand velocity. Quantitatively, however, the collected experimental data are in favor of

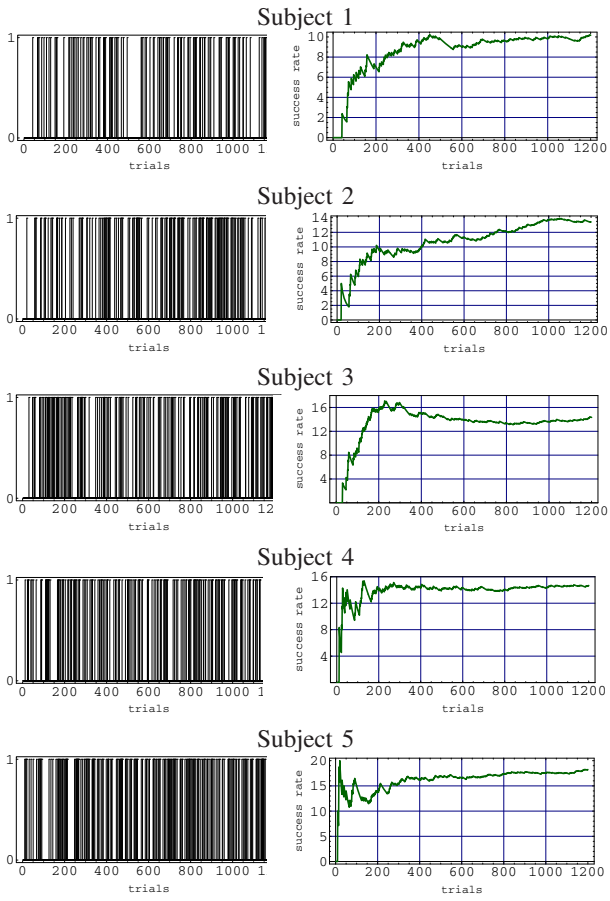

Fig. 4. Learning histories (left): black vertical lines correspond to successful trials. Evolution of the success rate (in percentages) as a function of the number of trials (right).

the optimization-based models, as the LOP models produce clearly visible overshoot in the range of 35-45%. As such, these models can be ruled out of consideration.

To determine which of the remaining models, MHJ or MHFC, produces a better match, we compared the models by the variance accounted for (VAF). This quantity shows how much of the signal variation is accounted for by a model, disregarding possible bias of the estimates [21]. The velocity VAF's for the hand and last bead predicted by the MHJ and MHFC models are drawn in the form of error bars (mean value plus/minus SD) in Figure 6. One can see that the MHFC model has an edge over the MHJ model.

It should be noted that overall the average VAFs for the hand are considerably lower than those for the last bead of the flexible object. There are several reasons that may explain it. First, the experimental hand velocities are noisier and have higher variances as they measured directly by the haptic device, while the bead velocities are obtained through the real-time simulation of the object dynamics. Second, the linear springs connected in cascade act as a mechanical filter attenuating higher frequencies of the input signal and sequentially (from the first to the last) smoothing the bead velocities. The third reason may be linked to the visual

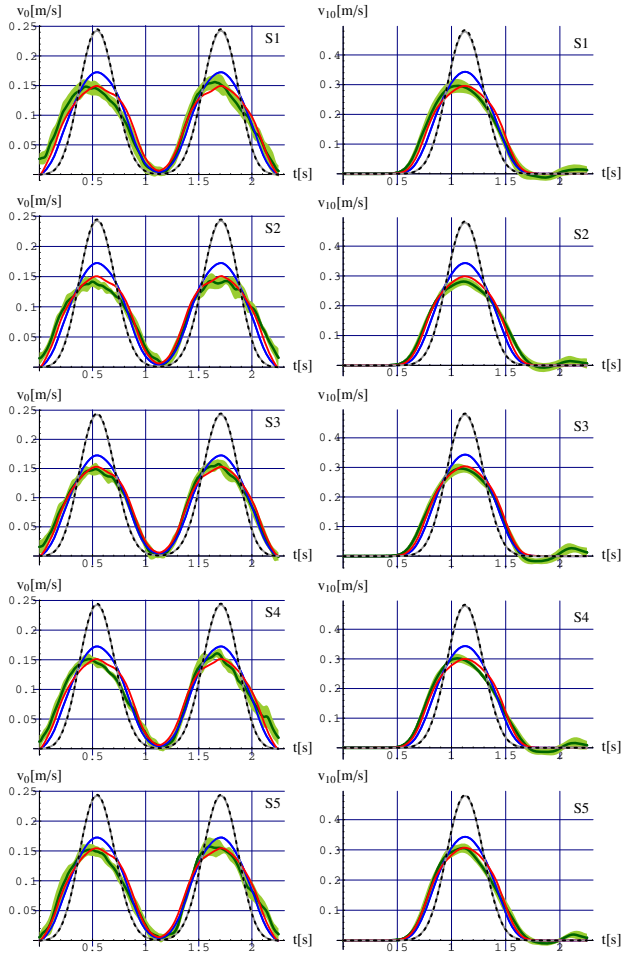

Fig. 5. Hand (left) and the last bead (right) velocity profiles, predicted by the MHJ (blue), the MHFC (red), the kinematic LOP (gray), and the dynamic LOP (dashed black) models in comparison with experimental data: mean values (dark green) are contoured by ± SD band (light green).

feedback. The hand position was displayed as a proxy point, not as a bead, and, comparing with the beads, it was more difficult for the subjects to trace it in performing the reaching movements.

V. Conclusions

An analysis of reaching movements in the manipulation of multi-mass flexible objects has been undertaken in this paper. Two theoretical approaches to modeling of reaching movements have been formulated for the cases of position and force-based actuation, resulting into four computational models. Theoretical predictions by the resulting four models have been tested against experimental data obtained with the use of a virtual reality-based setup. The experimental results show that, qualitatively, all the four models capture the non-trivial motion pattern featuring a double bell-shaped profile of the hand velocity. Quantitatively, however, the optimization-based models, the MHJ and MHFC ones, provide a significantly better prediction of the human movements, with the MHFC model outperforming the MHJ one

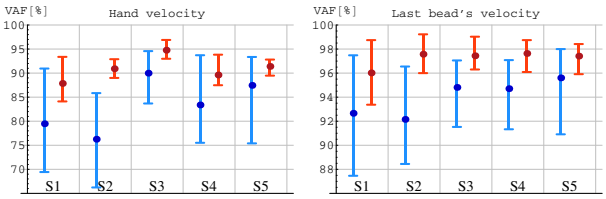

Fig. 6. VAFs for the hand (left) and the last bead (right) trajectory profiles, predicted by the MHJ (blue), the MHFC (red) models: mean values, shown with solid points, are contoured by min-max bars.

by a small margin.

To discriminate between the MHJ and MHFC models more convincingly, one can modify the dynamic environment, changing the parameters of the flexible object, its mass and stiffness. Note that the analytical structure of the solutions provided by these models, represented by combination of ordinary and trigonometric polynomials, admits, in principle, the existence of not only two-phased profiles but also those with three and more peaks. In principle, one can try to find a set of parameters producing two essentially different theoretical predictions, thus designing a critical test. However, one cannot ensure that the reaching movements in such a dynamic environment would be learnable in a reasonably affordable amount of time. In our opinion, this is one of the most difficult problems in designing critical tests and the corresponding experimental setups and protocols.

Our results demonstrate that the (currently available) generalizations of the concept of natural motion in analytical mechanics do not work well in the context of natural human movements. On the other hand, the optimization models of reaching movements do a better job in predicting experimental motion patterns.

Appendix

Typically, the human hand is modeled as a mass-damper-spring system, and this model holds for small movements and a short period of time. Based on this model, the hand impedance can be evaluated by perturbing the hand during maintenance of a given posture and measuring the hand displacement [22]–[24]. However, the use of this technique for a light weight haptic device without additional hardware, such as the one proposed in [25], is problematic.

A simple method, based on the accommodation to forced vibrations, can be constructed as follows. Assume that a human subject can follow the motion of a virtual object of mass m_1, connected to the hand by a spring of stiffness k and a damper of viscosity b, without developing his or her own driving force. Assume also that a periodic force of amplitude F and frequency Ω is applied to the hand, and the total haptic force is defined as

$$f_{\text{haptic}} = b(\dot{x}_1 - \dot{x}_0) + k(x_1 - x_0) + F\cos\Omega t. \qquad (34)$$

For a sufficiently high stiffness and low resistance the steady state solution to the system dynamics is developed as

$$x_0(t) \approx x_1(t) \approx \frac{F}{(m_0 + m_1)\Omega^2}\,(1 - \cos\Omega t)\,. \qquad (35)$$

By measuring the differences of the peak amplitudes for the hand and/or the object, $\Delta x_0, \Delta x_1$, one can estimate the hand mass from one of the following nonlinear (with respect to m_0) relationships:

$$\Delta x_0 \approx \Delta x_1 \approx \frac{2F}{(m_0+m_1)\Omega^2}. \tag{36}$$

Either of Δx_0 or Δx_1 can be used for the estimation of the hand mass m_0. Practically, however, it is more preferable to deal with Δx_1 as its measurement is less noisy.

In our experiments, the parameters of the haptic simulator were set as follows: $m_1 = 1\text{kg}, F = 1.8\text{N}, \Omega = \pi\,\text{rad/s}, k = 600\text{N/m}, b = 0.05\text{Ns/m}$. The haptic force along the movement line was computed by (34), while that in the lateral directions was modeled by a virtual spring of stiffness 600N/m. The object dynamics were simulated in the computer (the 4th-order Runge-Kutta method with constant step 0.001s). The subjects were requested to hold the PHANToM stylus at the configuration similar to the one they had used in the production of reaching movements in the previously completed experiments. The subjects were instructed not to resist the motion of the virtual object and follow it in the most comfortable mode, without exerting his own driving force or minimizing it as much as possible.

The positions of the hand (proxy point) and the object were displayed on the computer monitor. In addition to this standard visual feedback, a digital oscillograph was implemented in a pop-up window. Two signals were displayed on the digital oscillograph, the simulated object position and the reference signal (35), computed initially with $m_0 = 1\text{kg}$, and the simulated object position. The subjects were instructed to synchronize frequencies of these two signals. They could also incrementally adjust the amplitude of the reference signal (the reference value of m_0) by pressing up and down arrow buttons on the computer keyboard.

TABLE II
EFFECTIVE HAND MASSES m_0 [KG].

Subject	S1	S2	S3	S4	S5
Average	0.362	0.397	0.461	0.412	0.503
Minimum	0.108	0.162	0.242	0.127	0.201
Maximum	0.805	0.693	0.730	0.911	0.882
SD	0.156	0.131	0.108	0.174	0.149

Each subject underwent 20 trials, and each trial lasted, on average, 3 minutes. The samples of the differences of the peak amplitudes Δx_1 at the synchronized fragments of the reference and simulated signals were collected for analysis. The number of samples in each trial exceeds 50. The average, minimum, and maximum estimates of the hand mass are listed in Table II.

REFERENCES

[1] F. Pollick, J. Hale, and M. Tzoneva-Hadjigeorgieva, "Perception of humanoid movements," *International Journal of Humanoid Robotics*, vol. 2, no. 3, pp. 277–300, 2005.

[2] M. Gielniak, C. Liu, and A. Thomaz, "Generating human-like motion for robots," *The International Journal of Robotics Research*, vol. 32, no. 11, pp. 1275–1301, September 2013.

[3] T. Flash, Y. Meirovitch, and A. Barliya, "Models of human movement: Trajectory planning and inverse kinematics studies," *Robotics and Autonomous Systems*, vol. 61, pp. 330–339, 2013.

[4] T. Flash, N. Hogan, and M. Richardson, "Optimization principles in motor control," in *The Handbook of Brain Theory and Neural Networks*, 2nd ed., M. Arbib, Ed. Cambridge, Massachusetts: MIT Press, 2003, pp. 827–831.

[5] E. Todorov and M. Jordan, "Optimal feedback control as a theory of motor coordination," *Nature Neuroscience*, vol. 5, pp. 1226–1235, 2002.

[6] T. Flash and N. Hogan, "The coordination of arm movements: An experimentally confirmed mathematical model," *The Journal of Neuroscience*, vol. 5, no. 7, pp. 1688–1703, 1985.

[7] Y. Uno, M. Kawato, and R. Suzuki, "Formation and control of optimal trajectory in human multijoint arm movement. minimum torque-change model," *Biological Cybernetics*, vol. 61, pp. 89–101, 1989.

[8] P. Morasso, "Spatial control of arm movements," *Experimental Brain Research*, vol. 42, pp. 223–227, 1981.

[9] W. Abend, E. Bizzi, and P. Morasso, "Human arm trajectory formation," *Brain*, vol. 105, pp. 331–348, 1982.

[10] R. Plamondon, P. Alimi, A.M. Yergeau, and F. Leclere, "Modeling velocity profiles of rapid movements: A comparative study," *Biological Cybernetics*, vol. 69, pp. 119–128, 1993, jERK and SNAP.

[11] S. Engelbrecht, "Minimum principles in motor control," *Journal of Mathematical Psychology*, vol. 45, pp. 497–542, 2001.

[12] J. Dingwell, C. Mah, and F. Mussa-Ivaldi, "Experimentally confirmed mathematical model for human control of a non-rigid object," *Journal of Neurophysiology*, vol. 91, pp. 1158–1170, 2004.

[13] D. Aspinwall, "Acceleration profiles for minimizing residual response," *ASME Journal of Dynamic Systems, Measurement, and Control*, vol. 102, no. 1, pp. 3–6, March 1990.

[14] B. Karnopp, F. Fisher, and B. Yoon, "A strategy for moving a mass from one point to another," *Journal of the Frankline Institute*, vol. 329, no. 5, pp. 881–892, May 1992.

[15] A. Piazzi and A. Visioli, "Minimum-time system-inversion-based motion planning for residual vibration reduction," *IEEE/ASME Transactions on Mechatronics*, vol. 5, no. 1, pp. 12–22, March 2000.

[16] J. Lévine and D. Nguyen, "Flat output characterization for linear systems using polynomial matrices," *Systems & Control Letters*, vol. 48, no. 1, pp. 69–75, January 2003.

[17] M. Svinin, I. Goncharenko, Z. Luo, and S. Hosoe, "Reaching movements in dynamic environments: How do we move flexible objects?" *IEEE Transactions on Robotics*, vol. 22, no. 4, pp. 724–739, August 2006.

[18] S. Morita, "Trajectory generation between two arbitrary states based on hamilton's principle: A variable substitution method," *International Journal of Humanoid Robotics*, vol. 9, no. 3, 2012.

[19] S. Soltakhanov, M. Yushkov, and S. Zeghda, *Mechanics of Nonholonomic Systems: A New Class of Control Systems*, ser. Foundations of Engineering Mechanics. Berlin: Springer-Verlag, 2009.

[20] A. Newell and P. Rosenbloom, "Mechanisms of skill acquisition and the law of practice," in *Cognitive Skills and Their Acquisition*, J. Anderson, Ed. NJ: Erlbaum: Hillsdale, 1981, pp. 1–55.

[21] R. Toth, *Modeling and Identification of Linear Parameter-Varying Systems*, ser. Lecture Notes in Control and Information Sciences. Berlin Heidelberg: Springer-Verlag, 2010, vol. 403.

[22] T. Tsuji, P. Morasso, K. Goto, and K. Ito, "Human hand impedance characteristics during maintained posture in multi-joint arm movements," *Biological Cybernetics*, vol. 72, pp. 475–485, 1995.

[23] J. Speich, L. Shao, and M. Goldfarb, "Modeling the human hand as it interacts with a telemanipulation system," *Mechatronics*, vol. 15, pp. 1127–1142, 2005.

[24] P. Marayong, G. Hager, and A. Okamura, "Effect of hand dynamics on virtual fixtures for compliant human-machine interfaces," in *14th Int. Symposium on Haptic Interfaces for Virtual Environment and Teleoperator Systems*, Alexandria, Virginia, March 25-26 2006, pp. 109–115.

[25] M. Fu and M. Çavuşoğlu, "Human-arm-and-hand-dynamic model with variability analyses for a stylus-based haptic interface," *IEEE Trans. on Systems, Man, and Cybernetics, Part B (Cybernetics)*, vol. 42, no. 6, pp. 1633–1644, December 2012.